

# **Original Research Article**

## **New Dimension to the Physicochemical Characteristics of Ogwuta Source Clay**

---

### **ABSTRACT**

**Aims:** One of naturally abundant minerals with diverse industrial applications is the clay mineral. The choice of application depends on the characteristics of the clay. In this study, the mineralogical and physicochemical properties of the large and untapped Ogwuta clay deposit located in Afikpo, South eastern Nigeria was investigated as a guide to its application.

**Study design:** This study was carried out by experiment and the use of analytical instruments.

**Place and Duration of Study:** This study was carried out at the Department of Pure and Industrial Chemistry, Faculty of Science, University of Port Harcourt. It lasted for a year and half months.

**Methodology:** Fourier Transform Infrared (FTIR), X-ray diffraction (XRD), Scanning Electron Microscope (SEM) and Thermogravimetric (TG) techniques were employed. The X-ray fluorescence (XRF) analyzer was used to access the metal oxide composition while the Cation Exchange Capacity (CEC) was determined using the methylene blue method.

**Results:** The result showed that the clay is acidic with a pH of 2.8 and low CEC of 18.8 meq/100g. Silica ( $\text{SiO}_2$ ), Alumina ( $\text{Al}_2\text{O}_3$ ),  $\text{Na}^+$ , and  $\text{K}^+$  of 48.62%, 19.08%, 4.67% and 1.05% respectively. The clay is limited in mineral impurities with 0.0%  $\text{T}^{4+}$ , 1.67%  $\text{Mg}^{2+}$ , and 0.34%  $\text{Ca}^{2+}$  but high in carbonaceous matter with loss on ignition (LOI) of 11.29%. XRD revealed kaolinite as the predominant mineral with the presence of quartz and polygorskite.

**Conclusion:** This study posits that the clay can be potentially suitable for the coating of paper, like other kaolinites, to enhance its printability and opacity.

*Keywords: Cation exchange capacity, silica, characterization, kaolinite, source clay*

### **1. INTRODUCTION**

According to the Clay Mineral Society, clay minerals are naturally occurring materials composed mainly of fine-grained minerals which become plastic in the presence of water and become hard when dried or fired. They are any group of hydrous aluminum silicates having diameter less than 0.005mm. This inherent size of clay crystallites is as a result of the amount of crystal defects in the axes of symmetry [1], which diminishes the crystal growth and making nucleation less energy consuming. They are mainly inorganic material formed by in situ weathering of parent minerals and by hydrothermal alteration of the host rocks [2]. Non crystalline hydroxides of metals such as Al, Fe, Mg, Ni etc. are capable of co-precipitating  $\text{SiO}_2$  from its dilute solution produced by weathering process. The concentration

of  $\text{SiO}_2$  relative to that of the cation in the weathered solution, more often determine the mineral type in the clay [3].

Basically, clays are made of complex silicates of various ions such as  $\text{Al}^{3+}$ ,  $\text{Fe}^{2+}$ ,  $\text{Mg}^{2+}$  etc. due to the importance of water to clay formation, they are often regarded as hydrous aluminosilicates or hydrous aluminum phyllosilicates [4]. Iron substitute for aluminum and magnesium to varying degrees and appreciable quantity of potassium, sodium and calcium are frequently present [5]. Structurally, clay minerals like all phyllosilicates are characterized by two dimensional sheets of corner sharing  $\text{SiO}_4$  tetrahedra and/or  $\text{AlO}_4$  octahedra. The silicon-oxygen tetrahedral consists of silicon surrounded by four oxygen atoms that unite to form the silica sheet. The aluminum or magnesium octahedron consists of aluminum surrounded by six hydroxyl units to form the gibbsite or brucite sheet, depending on any of the dominating atoms. The tetrahedral sheet has  $\text{Si}^{4+}$  surrounded by three basal oxygen atoms shared by three other nearby tetrahedral sheets. The fourth free oxygen atom (known as apical oxygen) forms bond or link with other tetrahedral or octahedral sheets [6]. The tetrahedral sheet is charge deficient due to the isomorphous substitution of  $\text{Al}^{3+}$  in place of  $\text{Si}^{4+}$ . Conversely, the predominant metal ion in the octahedral sheets are  $\text{Al}^{3+}$  and  $\text{Mg}^{2+}$  that are surrounded by six oxygen or hydroxyl group. Aluminum, with three positive valences, has only two-thirds of the sites filled.

This results in the formation of a di-octahedral sheet  $[\text{Al}_2(\text{OH})_6]$ . If magnesium ion dominates, a tri-octahedral sheet, with unit cell formula,  $\text{Mg}_2(\text{OH})_6$  is formed through the sharing of two oxygen of each octahedral. The sheet units have the chemical composition  $(\text{AlSi})_3\text{O}_4$ .

Different clays have different ways these layers of sheets are packed or arranged. Consequently, clays are categorized depending on the tetrahedral-octahedral sheet sequence. If there is only one tetrahedral and one octahedral in each layer, the clay is known as a 1:1 (T–O) clay. The other composition known as 2:1 (T–O–T) clay, has two tetrahedral sheets with the unshared vertex of each sheet pointing toward each other and forming each side of the octahedral sheet.

Based on their structures and chemical compositions, the clay minerals can be divided into four main classes of kaolinite, smectites, illites and micas [4]. However, Sarkar *et al.* [7] and Walter [8] refer to two or three classes of clays since illites are sometimes referred to as a 2:1 layer and not a 2:1:1. Also, illites/micas are sometimes grouped with smectites. Clays have particle size less than  $2\mu\text{m}$  and are distinguished from other fine-grained particles such as silt by their plasticity properties. Most clay particles are characterized by high swelling capacity, large specific surface area and high cation exchange capacity [9]. Kaolinites on the other hand have low shrink-swell capacity and a low cation exchange capacity (1-15 meq/100g) with a triclinic crystal system and specific gravity of 2.16-2.68.

These properties make clay minerals find wide applications. They are useful as an annular seal or plug for water wells and as protective liner for landfills. Other uses include as an anti-caking agent in animal feed. In paper making, they are mixed with cellulose fiber to give it body, opacity and printability. In the oil and gas industry, montmorillonite is a major component of the drilling mud which helps in keeping the drill bit cool and removing drilled solids (Stanisa *et al.* [10]. The endothermic dehydration of kaolinites produces disordered metakaolin which is a complex amorphous compound that when added to concrete mix, accelerates the hydration of Portland cement [11]. Bhattacharyya and Gupta [12] added that they are effective as an adsorbent for the removal of heavy metals. This is possible because clay minerals have a net negative charge due to the isomorphous substitution of silicon ion by aluminum ion in the tetrahedral layers or likely substitution of aluminum ion by magnesium ion.

There are several clay deposits in Nigeria ranging from the North to the East (both identified and unidentified). It is therefore imperative that these clay minerals be x-rayed in physical, chemical, thermal, refractory properties and documented for immediate and future use.

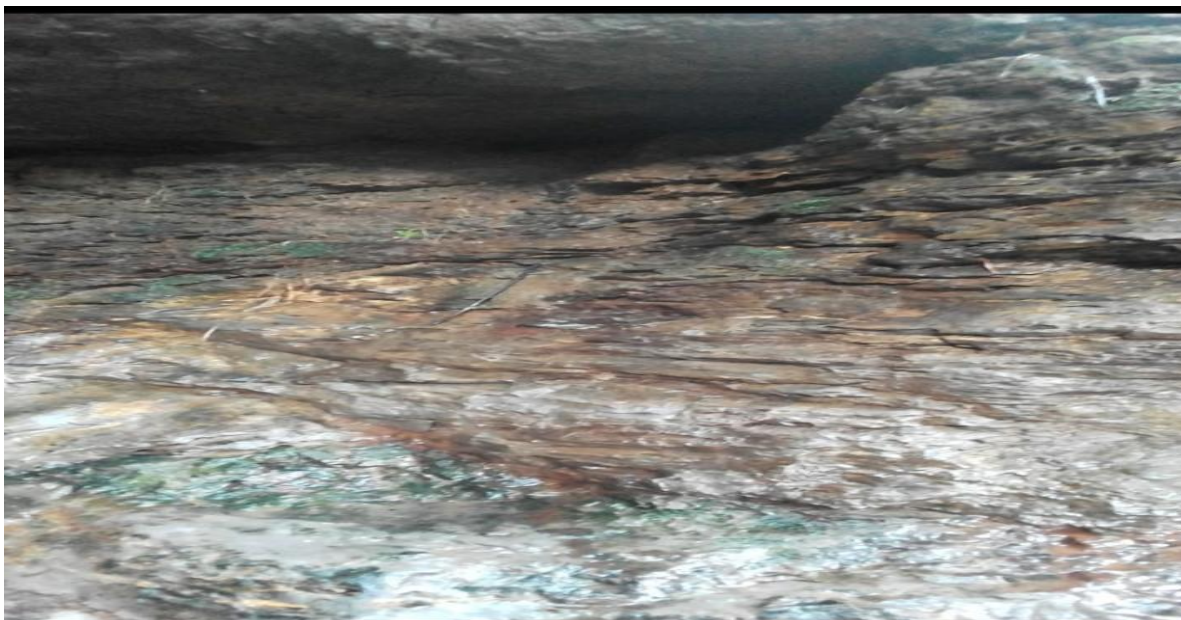


**Plate 1.** Ogwuta clay deposit

In this study, the physicochemical characterization of source clay from Unwana, Afikpo, South Eastern part of Nigeria was carried out to assess its properties and predominant mineral present. The deposit covers large expanse of land with little or no knowledge of its properties for possible exploration. X- ray fluorescence (XRF), Fourier Transform infra-red (FTIR), X-ray diffraction (XRD), and Thermogravimetric analysis (TGA), among other parameters, were employed in the analysis.

## **2. MATERIAL AND METHODS**

### **2.1 Materials**

The clay sample was collected from its natural deposit 12 cm below earth surface in Unwana, a community in Afikpo North Local Government Area of Ebonyi State, South Eastern Nigeria (N 5° 47' 38.154", E 7° 55' 56.538"). The sample was sun-dried for 2-3 days. The impurities found on the clay sample were removed by hand. The sample was further oven- dried at 105°C for 2 hrs using BTOV 1423 oven, crushed with an iron roller to fine particle sizes. These clay particles were sieved into 63 µm size and stored in a glass bottle.

### **2.2 Methods**

#### **2.4 Sample Characterization**

##### ***2.4.1 pH Determination***

A 50 ml of deionized water was added to 10 g of the clay sample in a 250 ml beaker in the ratio of 1:5 of clay to water. The mixture was stirred with glass rod and allowed to stand for 30 min and the pH taken.

#### 2.4.2 Surface Area Determination of the Sample

The surface area of the clay sample was determined according to the method of Alvarez *et al.* [13]. A 1.5 g of clay sample was agitated in 100 ml of dilute HCl, that had been diluted to pH of 3.0. Then, 30 g of NaCl was added while stirring the suspension. The volume was made up to 150 ml with deionized water, resulting in the change of pH to 4.0. A 0.1M NaOH was used to raise the pH from 4.0 to 9.0 and the volume (V) of NaOH used was recorded. The surface area  $s$ , was calculated using the equation:

$$S = 32V - 25 \quad (1)$$

#### 2.4.3 Specific Gravity Determination of Clay Sample

This was determined using the Archimedes principle described by Dada *et al.* [14]. Briefly, the weight of an empty 50 ml specific bottle ( $w_1$ ) was measured on a weighing balance. Then the bottle was filled with water and the weight ( $w_2$ ) measured. The clay sample (10 g) was added to an empty dry specific bottle and the weight ( $w_3$ ) recorded. Finally, the bottle containing the sample was then filled with water and all air bubbles expelled before the weight ( $w_4$ ) was measured. The specific gravity (s.g) of the clay was calculated as below:

$$\text{s.g} = \frac{\text{weight of sample}}{\text{weight of equal volume of water}}$$
$$\text{s.g} = \frac{w_3 - w_1}{(w_2 - w_1) - (w_4 - w_3)} \quad (2)$$

#### 2.4.4 Determination of Total Pore Volume

The total pore volume of the clay sample was determined by boiling 20 g of the sample immersed in water. After the air in the sample had been displaced, the sample was superficially dried and weighed. The total pore volume was calculated as increase in weight divided by the density of the water ( $1 \text{ g/cm}^3$ ).

#### 2.4.5 Cation Exchange Capacity Determination of Clay Sample

The cation exchange capacity of the clay was determined according to the standard test method for methylene blue index for clay designated by C837-09. A 2.0 g of previously dried clay was placed in 1L beaker containing 300 ml of water. The mixture was stirred until uniform dispersion was achieved. The pH of the slurry was determined and sufficient sulphuric acid added to bring the range to within 2.5 - 3.8. With the slurry still under the mixer, 5 ml of 0.01N methylene blue solution was added and stirred for 1-2 min. With the help of a dropping pipette, a drop of the slurry was made on the edge of a filter paper and the appearance of the drop observed. This continued until the endpoint marked by the appearance of a light blue halo around the drop. The Methylene Blue Index (MBI) was calculated thus:

$$\text{MBI} = \frac{0.01 \times V}{2} \times 100 \quad (3)$$

Where V represents the volume, in mL of the methylene blue solution required for the titration.

#### 2.4.6 Metal Oxide Composition Determination

This was done using a combination of the wet and the dry methods. Oxides of K, Al, Mg, Fe, Ca and Na were analyzed using XRF Analyzer (DCC-6000 Mineral mode).

Silicon dioxide (SiO<sub>2</sub>) was analyzed according to the method of Costanzo [15]. Briefly, 1.0 g of the sample was washed three times with a homo-ionic solution of 1M NH<sub>4</sub>Cl and then with a 50% (v/v) mixture of ethanol and distilled water until the supernatant solution is free of Cl<sup>-</sup> by the AgNO<sub>3</sub> method. The sample was oven-dried overnight at 105°C. The elemental composition of the sample was determined following digestion with analytical grade aqua regia and boric acid in an oven using platinum crucible. The oxide was determined using Atomic Absorption Spectrophotometer. The loss on ignition (LOI) was determined by burning 1.0 g of samples at 1000°C in a muffle furnace.

#### **2.4.7 Fourier Transform Infra-Red (FTIR) of Clay Sample**

A 1.0 mg of the sample was mixed with a little quantity of KBr in the ratio of 1:10 (1 mg: 10 mg) and finely pulverized in an agate mortar with pestle to homogenize the mixture. A little amount of the mixture was placed in a miniature press and compressed to form a disc or pellet of about 1mm thickness. This was placed in the appropriate sample holder, the holder, with sample, was mounted on the sample compartment of the FTIR Spectrometer. The system was set to make 16 scans within 4000 cm<sup>-1</sup> to 400 cm<sup>-1</sup> and on completion of the scan, the spectrum was displayed on the 'view' window automatically. The individual peaks on the spectrum were labeled with their corresponding wavelengths and the spectrum printed out.

#### **2.4.8 Scanning Electron Microscope (SEM)**

SEM for the clay samples was done according to the method reported by Rajkumar *et al.* [16].

#### **2.4.9 Thermogravimetric Analysis**

The thermal analysis of the clay sample was done using a simultaneous TGA-DTA (Pekin Elmer TGA 4000) analyzer. Approximately 11.209 mg of powder sample was loaded into the platinum sample pan and heated from ambient temperature to 950°C at a heating rate of 10°C/min under air purge gas drawn at 20 ml/min and pressure of 2.5 bar. Traces were recorded as percentage weight loss versus temperature.

### **3. RESULTS AND DISCUSSION**

From Table 1, the pH of the clay samples at 30°C was 2.8, indicating the sample was acidic. Generally, the acidic value of clay can largely be accounted for by the composition of the parent rock-material from which it was formed and partly by environmental factors such as rainfall [17], that is, clay samples from areas with lots of rainfall have pH values less than 3.5. The result agrees with the observation by Suedina and Carla [18] that clays have 0.67 units of negative charge per unit cell resulting from the isomorphous substitution of Al<sup>3+</sup> by Mg<sup>2+</sup> and Si<sup>4+</sup> by Al<sup>3+</sup>. Consequently, they behave as weak acids with pH values less than 4.

**Table 1.** Some physical properties of clay used in this work

<b>Parameter</b>	<b>Natural Clay</b>
------------------	---------------------

---

pH	2.8
Surface Area	133.4m <sup>2</sup> g <sup>-1</sup>
Specific Gravity	2.16gcm <sup>-3</sup>
Pore Volume	0.45m <sup>3</sup> g <sup>-1</sup>
CEC	18.8meq/100g

---

### **3.1 Specific Surface Area**

The specific surface area was found to be 133.4 m<sup>2</sup>g<sup>-1</sup>. This shows that the sample is made of fine particles. According to Uzochukwu [19], after measuring the surface area of some clay samples using Ethylene Glycol Monoethyl Ether method, submitted that Finer particles of a given sample pose values that are higher than coarser particles. Specific surface area values range from 50 m<sup>2</sup>/g to as high as 736 m<sup>2</sup>/g in silica - bonded montmorillonite [20].

### **3.2. Specific Gravity**

The specific gravity was found to be 2.16 g/cm<sup>3</sup>. This value falls within the range of a minimum of 1.8 to a maximum of 2.6 for clays [21]. The value was comparable to the clay from Ihitte Obama with value 2.14 [22] and those from Abakaliki area with values 2.23 and 2.28 [23].

### **3.3. Cation Exchange Capacity**

The cation exchange capacity of the clay was determined to be 18.8 meq/100g at pH 6. This property of clay arises from isomorphous substitution, a crystal lattice defect in which a given ionic series may be replaced by another in a crystal lattice, [24]. According to Neeraj and Chandra [4], values of CEC range from 3-15 in kaolinites through 15-40 in chlorites and illites, 70-100 in montmorillonite and 100-150 in vermiculite.

### **3.4. Metal Oxide Composition**

The results of the metal oxide composition of the clay as presented in Table 2 showed that the alumina and silica oxide was in major quantity. The high iron oxide content of over 6 % was consistent with other local clays such as Oboro and Abakaliki [23]. The loss on ignition value of 11.29 % revealed that the clay was high in carbonaceous matter [25]. Also, the percentage composition of Mg, Ca, Na and K were 1.62, 0.34, 4.67, and 1.05 respectively are considered substantial. Noted was the considerable amount of iron suggesting the presence of impurities, which was commonly seen in clays formed from soils under tropical conditions [26]. However, with zero Ti content and less than 2 % Mg and Ca content, the clay showed limited mineral impurities [27].

**Table 2.** Metal oxide compositions (%) of the clay used in the study

Element	Natural Clay
Al	19.08
Si	48.62
Mg	1.62
Ca	0.34
Na	4.67
K	1.05
Fe	6.99
Ti	0.00
Cl <sup>-</sup>	0.57
LOI	11.29
Moisture	0.55

### 3.4. Scanning Electron Microscope (SEM)

The Scanning Electron Micrograph of the clay, as presented in Figures 1 revealed particles formed by large agglomerates of irregular sizes and shapes. The agglomeration arises from the tendency by clay particles to repel each other electrostatically, depending on the ion density and inter-granular distance [28]. However, Mitchell and Soga [29] noted that breaking of the clay material can expose hydroxyl group, leading to the existence of hydrogen bond. This will ultimately bring about clumping of particles which can be seen as edge-to-edge, edge-to-face or face-to-face flocculation.

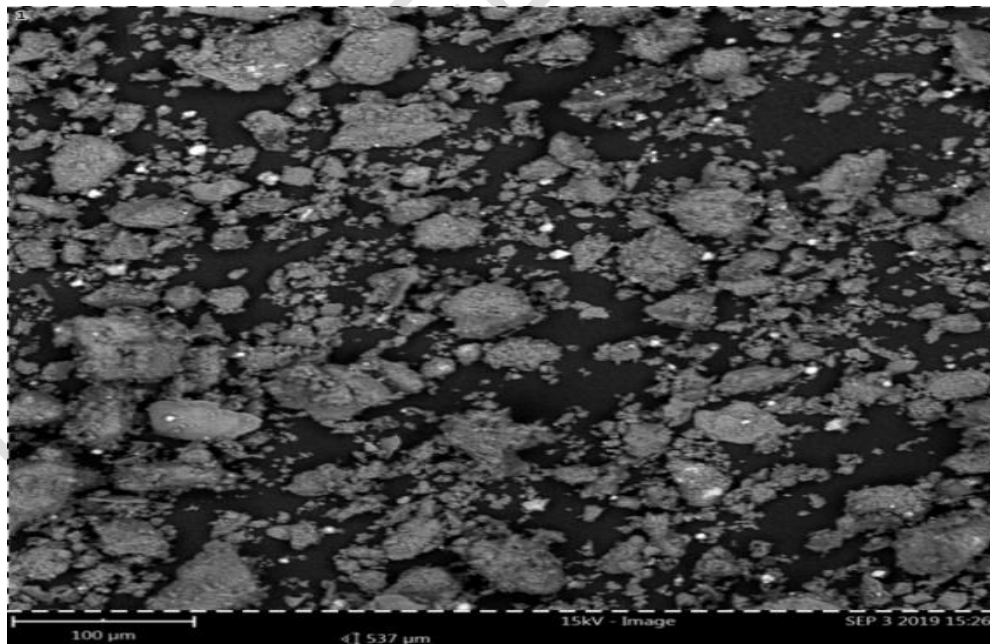


**Fig. 1.** SEM image of natural clay

### **3.5. Thermal Analysis**

The thermal behavior of the clay sample, as presented in Figure 2 showed thermal behavior similar to most kaolinitic clay samples in literature [30, 31]. It showed initial exothermic weight gain that peaked at 39.84°C. This might be attributed to hygroscopic behavior of the samples enhanced by not using very dried air [32]. However, all gained weight was lost completely at 45.51°C. Also, the sample exhibited characteristic exothermic weight loss (2 %) around 100-150°C. This could be associated with the physically adsorbed water [33]. From 153-325°C, the observed weight percent loss (13.67 %), consistent with kaolinitic clays, was due to the removal of water of crystallization of the interlayer cations [34]. The last step of weight loss was observed between 532°C and 776°C which, according to Conconi *et al.* [31] was due to the dehydroxylation of the hydroxyl group of the natural clay sample.

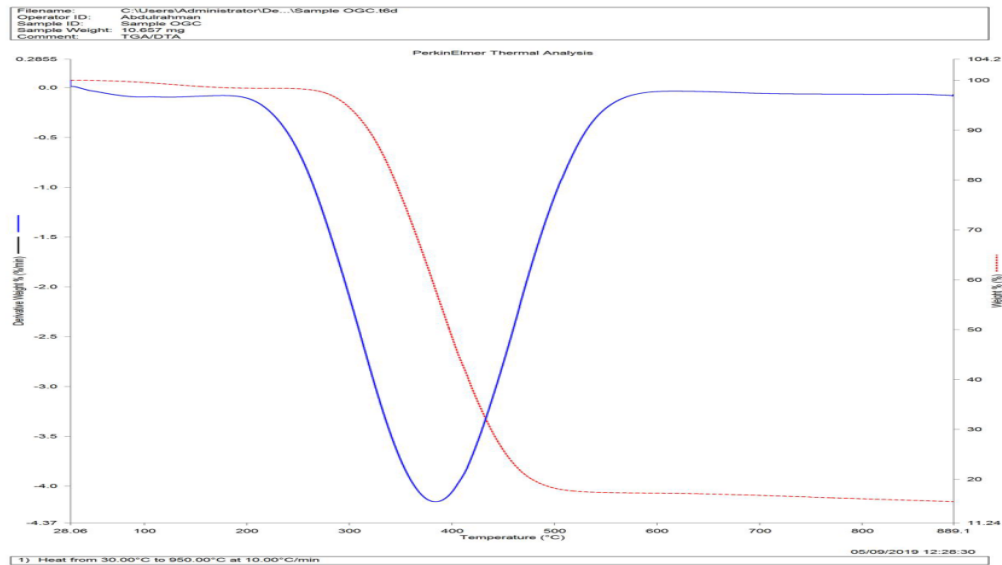


**Fig. 2.** TGA/DTA of natural clay sample

### **3.6. X-Ray Diffractogram**

Clay materials are made of layers of silicates. To study the interlayer distance, the X-ray diffractometry (XRD) was employed. The sample clay was subjected to this method. The  $d_{001}$  peak displacements as shown in Figures 3a-3c showed a basal spacing of 7.13Å at a  $2\theta$  angle of 14.115°. This also shows that clay sample has a well-defined characteristic of most

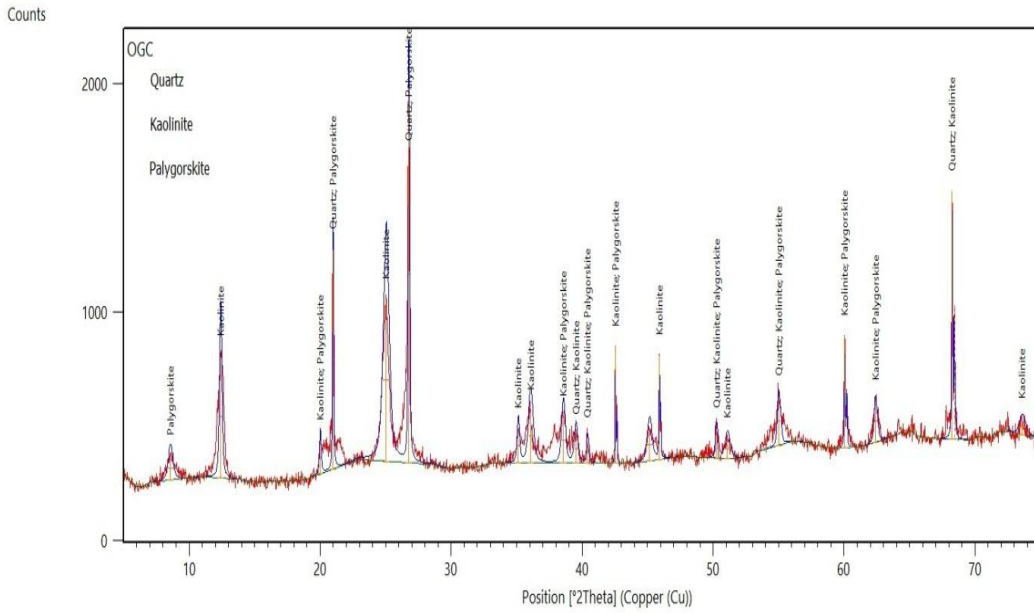


Fig. 3a. XRD spectrum of natural clay sample

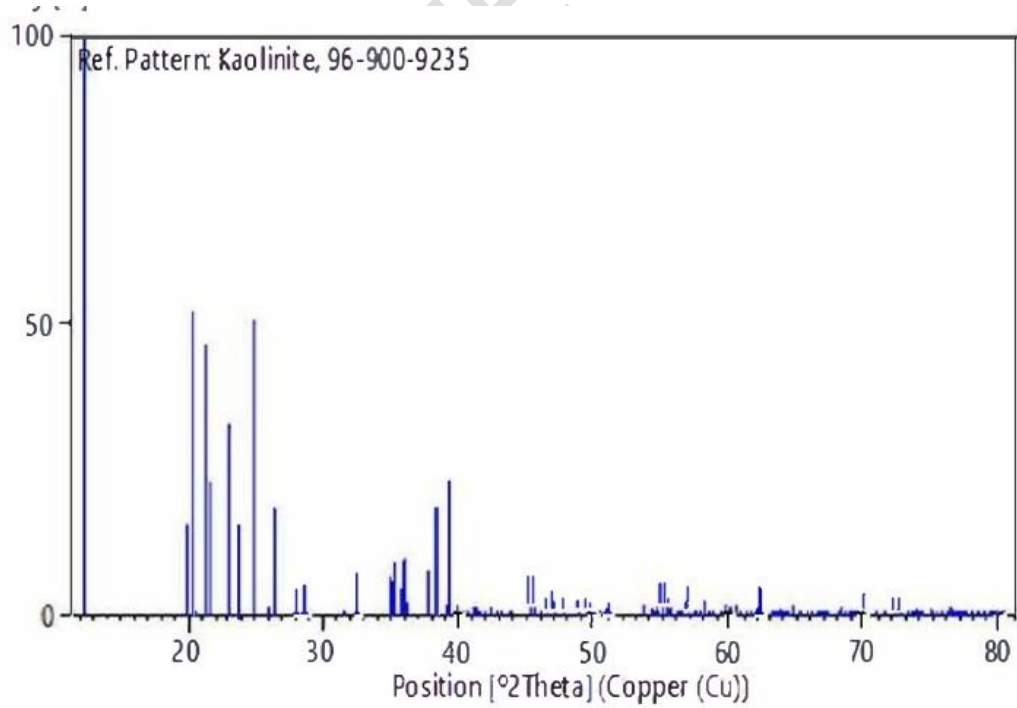
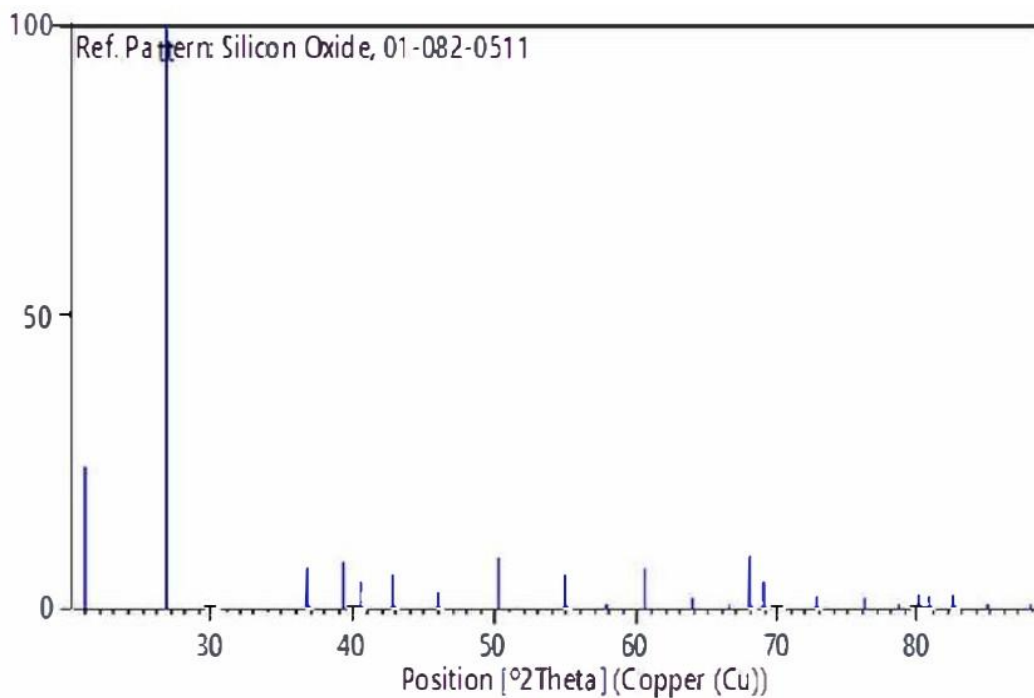


Fig. 3b. XRD Stick Pattern for clay kaolinite mineral



**Fig. 3c.** Stick pattern showing silicon oxide

**Table 3.** Interlayer spacing of unmodified natural clay

Sample	d(Å)	2θ(°)
Natural clay	7.134	14.115

### 3.7 FTIR Spectrum

The Fourier Transform Infra-Red spectra and the vibrational band assignment of the sample as presented in Figure 4 and Table 4 respectively revealed that the peak at  $671.25\text{ cm}^{-1}$  was due to Al-O-Si stretching while that at  $771.55\text{ cm}^{-1}$  belongs to the Al-O-Fe bending in quartz [36]. The inner surface hydroxyl group (Al-OH-Al) deformation band was observed at  $918.15\text{ cm}^{-1}$  and the bands associated with Si-O stretching, characteristic of kaolinite was  $1010.75\text{ cm}^{-1}$ . Kaolinite  $\text{H}_2\text{O}$  bending bands for the sample was observed at  $1635.69\text{ cm}^{-1}$ , while water molecule stretching characteristic of montmorillonite was observed at  $3356.25\text{ cm}^{-1}$  [37].

**Table 4.** Vibrational bands natural clay sample

S/N	Natural Clay	Assignment
1	671.25	Al-O-Si stretching
2	771.55	Al-OH-Fe bending in quartz
3	918.15	Al-OH-Al bending (deformation of inner surface hydroxyl group)
		Si-O stretching in Kaolinite
4	1010.75	H-O-H bending
5	1635.69	H-O-H bending from Inner octahedral Al-OH
6	3356.25	OH stretching in Kaolinite
7	3626.29	

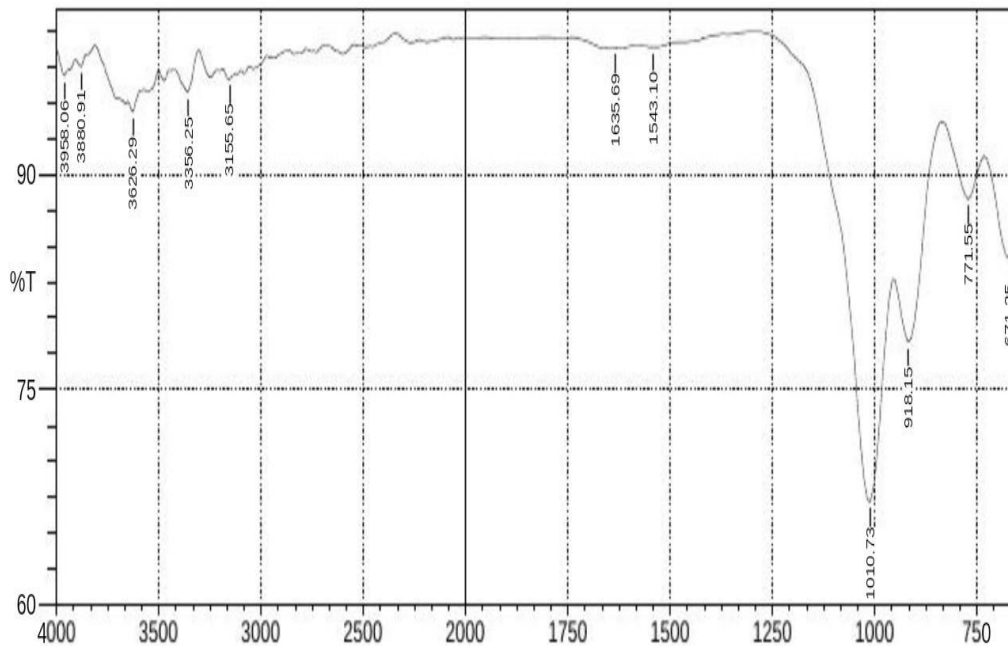


Fig. 4. FTIR spectrum of natural clay sample

#### 4.0 Conclusion

Local clay sample was sourced from its vast natural deposit and characterized for proper classification and determination of possible application. Both classical and spectroscopic techniques were employed. A combination of wet and dry methods was used to determine the metal oxide composition which showed 48.62% and 19.08% of silica ( $\text{SiO}_2$ ), and alumina ( $\text{Al}_2\text{O}_3$ ) respectively. The XRD analysis confirmed kaolinite as the predominant mineral, with the presence of polyhgorskite and quartz. The temperature behavior of the clay as shown by the thermogravimetric result further confirmed kaolin as the dominant argillaceous mineral in the form of hydrated alumino silicate given the 13.69% water of crystallization. Also, the 0.0%  $\text{T}^{4+}$  content and low  $\text{K}^+$ ,  $\text{Na}^+$  and  $\text{Mg}^{2+}$  content, show that the clay has limited mineral impurities. The high  $\text{Fe}_2\text{O}_3$  content of 6.99% is consistent with most clay formed in the tropics.

#### COMPETING INTERESTS DISCLAIMER:

**AUTHORS HAVE DECLARED THAT NO COMPETING INTERESTS EXIST. THE PRODUCTS USED FOR THIS RESEARCH ARE COMMONLY AND PREDOMINANTLY USE PRODUCTS IN OUR AREA OF RESEARCH AND COUNTRY. THERE IS ABSOLUTELY NO CONFLICT OF INTEREST BETWEEN THE AUTHORS AND PRODUCERS OF THE PRODUCTS BECAUSE WE DO NOT INTEND TO USE THESE PRODUCTS AS AN AVENUE FOR ANY LITIGATION BUT FOR THE ADVANCEMENT OF KNOWLEDGE. ALSO, THE**

**RESEARCH WAS NOT FUNDED BY THE PRODUCING COMPANY RATHER IT WAS FUNDED BY PERSONAL EFFORTS OF THE AUTHORS.**  
**REFERENCES**

1. Meunier A. Why are Clay Minerals Small? *Clay Miner.* 2018; 41(2): 551-566.
2. Li S, He H, Tao Q, Zhu J, Tan W, Ji C, Yang Y, Zhang C. Kaolinization of 2:1 Type Clay Minerals with Different Swelling Properties. *American Mineralogist*, 2020; 105(5): 687-697.
3. Herman H. Clay Mineral Formation Under Lateritic Weathering Conditions, *Clay Miner.* 2018; 12(4): 281-288.
4. Neeraj K, Chandra M. Basics of Clay Minerals and Their Characteristic Clay and Clay minerals. DOI: 10.5772/intechopen.97672, 2021.
5. Moore D, Reynolds RC. X-Ray Diffraction and the Identification and Analysis of Clay Minerals. 2<sup>nd</sup> edition. New York, Oxford University Press., 1997.
6. Ombaka O. Characterization and Classification of Clay Minerals for Potential Applications in Ragi Ward, Kenya. *Afri. J. Environ. Sci. Technol.* 2016; 10(11): 415-431.
7. Sarkar B, Singh MM, Mandal S, Churchmen G, Bolan S. Organic Matter Interaction in Relation to Carbon Stabilization in Soil: The Future of Soil Carbon. *Clay Miner.* 2018; 71-86
8. Walter IP. Economic Geology: Principles and Practice, 5<sup>th</sup> Ed. Washington, John Wiley & Sons, 2011.
9. Claudiane O, Rod J, Abir A. Comparison between Grannlar Pillared Organobentonites for Hydrocarbon and Metal Ion Adsorption. *Appl. Sci.* 2012; 67: 91-98.
10. Stanisa TS, Ivana MS, Ivan MS, Dragoljub G. Industrial Application of Clays and Clay Minerals. In *Clays and Clay Minerals: Geological Origin, Mechanical Properties and Industrial Applications*. Eds. Wesley Nova, 2014; 379-402.
11. Levista T, Gehor S, Eijarvi E, Sarpola A, Tanskanen J. Characteristics and Potential Applications of Coarse Clay Fractions from Puolance, Finland. *Central Euro J. Eng.* 2012; 2(2): 239-247.
12. Bhattacharyya GK, Gupta SS. Influence of Acid Activation of Kaolinite and Montmorillonite on Adsorptive Removal of Cd(II) Ion from Water. *Ind. Eng. Chem. Res.* 2008; 46(11): 3734-3742.
13. Alvarez AN, Rocha MC, Bertolino LC. Mineralogical Characterization of Natural Clay from Brazilian Southeast region for Industrial Application. *Ceramica*, 2017; 63(2017): 253-262.
14. Dada AO, Olalekan PA, Olatunya A. Langmuir, Freundlich Temkin and Dubinin-Radushkevich Isotherm Studies of Equilibrium Sorption of Zn<sup>2+</sup> Unto Phosphoric Acid Modified Rice Husk. *J. Appl. Chem.* 2012; 3(1): 38-45.
15. Costanzo PM 2001. Data and industrial minerals, including clay and clay mineral deposits. *J. Clay Clay Mater.* 2001; 59(5): 372-373.

16. Rajkumar U, Haunshi S, Paswan C, Raju MVLN, Rama RSV, Chatterjee RN. Characterization of indigenous Aseel chicken breed for morphological, growth, production and meat composition traits from India. *Poult. Sci. J.* 2017; 96:2120-2126.
17. Denis LG, Rubia RV, Claudio A. Adsorption of Thorium (IV) on Chemically Modified Amazon Clay. *J. Braz. Chem. Soc.* 2009; 20(6): 1164-1174.
18. Suedina ML, Carla RC. Application of Infrared Spectroscopy to Chitosan/Clay Nano Composites. *Infra-red Spectroscopy - Material Science, Engineering and technology.* Theophanides Theophile (Ed). Shanghai. Intech Publishing, 2012.
19. Uzochukwu CU. Measurement of Surface Area of Modified Clays by Ethylene Glycol Monoethyl Ether Method. *Asian J. Chem.* 2017; 29(9): 1891-1896.
20. Ahmet RM, Angel FC. Baseline Studies of the Clay Mineral Society, Chemical Analysis of Major Elements. *Clays Clay Miner.* 2010; 51(5): 381-386.
21. Dominique R, Françoise E. Characterization of Soil Clay Minerals. *Clays Clay Miner.* 1996; 44(6): 791-800.
22. Obi C. Adsorption studies of some clay minerals in Okigwe Local Government Area of Imo State. An M.Sc Thesis, University of Port Harcourt, 2006.
23. Nweke ES., Ugwu EI. Analysis and Characterization of Clay Soil in Abakaliki, Nigeria. *The Pacific J. Sci. Technol.* 2007; 8(2): 190-193.
24. Bergaya F, Vayer M. CEC of Clays: Measurement by Adsorption of a Copper Ethylenediamine Complex. *Appl. Clay Sci.* 2009; 12: 275-280.
25. Pushpaaletha P, Rugmini S, Latithambika M. Correlation between Surface Properties and Catalytic Activity of Clay Catalysts. *Appl. Clay Sci.* 2005; 30(1): 141-153.
26. Nnuka EE, Enejo C. Characterization of Nahuta Clay for Industrial and Commercial Application. *NJEM*, 2001; 2(3): 9-13.
27. Umbugadu A, Igwe O. Mineralogical and Major Oxide Characterization of Panyam Clays, North Central Nigeria. *Inter. J. Phys. Sci.* 2019; 14(11): 108-115.
28. Ural N. The Significance of Scanning Electron Microscope (SEM) analysis on the Microstructure of Improved Clay: An overview. *Open Geosci.* 2021; 13(1): 197-218.
29. Mitchel JK, Soga K. *Fundamentals of Soil Behaviour*. 3<sup>rd</sup> Ed. Hoboken. John Wiley & Sons, 2005.
30. Hassan UJ, Abdu SG. Structural Analysis and Surface Morphology of Kaolin. *Sci. World J.* 2014; 9(3): 33-37.
31. Conconi MS, Morosi M, Maggi J, Zaiba P, Cravero F, Rendtoff N. Thermal Behaviour (TG-DTA-TMA) Sintering and proportion of Kaolinitic Clay from Buenos Aires. *Ceramica*, 2019; (65): 374-379.
32. Tadele AS, Fikiru T. Synthesis and Characterization of Ethiopian Kaolin for the Removal of Basic Yellow (BY-28) dye from Aqueous Solution. *Helyon*, 2010; 6.

33. Wang H, Li C, Peng Z, Zhang S. Characterization and Thermal Behaviour of Kaolin. *J. Therm. Anal. Calori.* 2011; (105): 157-160.
34. Alejandra T, Monica AT, Alberto NS, Edgardo FI. Thermal analysis to assess pozzolanic activity of calcined kaolinitic clays. *J. Therm. Anal. Calorim.* 2014; 117: 547-556.
35. Okoye IP, Obi C. Synthesis and Characterization of Al-pillared Bentonite clay minerals. *Res. J. Appl. Sci.* 2011; 6 (7-12): 447-450.
36. Alemayelu K, Gholap A, Giovanni E. Fourier Transform Infrared Spectroscopic Characterization of Clay Minerals from Rocks of Lalibela Churches, Ethiopia. *Inter. J. Phys. Sci.* 2013; 8(3): 109-119.
37. George-Ivo EE. Fourier Transform Infrared Spectrophotometry as a Complementary Technique in Characterizing Clay Size Fractions of Kaolin. *J. Appl. Sci. Environ. Manage.* 2005; 9(2): 43-48.

UNDER PEER REVIEW